

# A New Tool for NMR Crystallography: Complete $^{13}\text{C}/^{15}\text{N}$ Assignment of Organic Molecules at Natural Isotopic Abundance Using DNP-Enhanced Solid-State NMR

Katharina Märker,<sup>†,§</sup> Morgane Pingret,<sup>†,§</sup> Jean-Marie Mouesca,<sup>†,§</sup> Didier Gasparutto,<sup>†,§</sup> Sabine Hediger,<sup>†,§,‡</sup> and Gaël De Paëpe<sup>\*,†,§</sup>

<sup>†</sup>Univ. Grenoble Alpes, INAC, F-38000 Grenoble, France

<sup>§</sup>CEA, INAC, F-38000 Grenoble, France

<sup>‡</sup>CNRS, SCIB, F-38000 Grenoble, France

**S** Supporting Information

**ABSTRACT:** NMR crystallography of organic molecules at natural isotopic abundance (NA) strongly relies on the comparison of assigned experimental and computed NMR chemical shifts. However, a broad applicability of this approach is often hampered by the still limited  $^1\text{H}$  resolution and/or difficulties in assigning  $^{13}\text{C}$  and  $^{15}\text{N}$  resonances without the use of structure-based chemical shift calculations. As shown here, such difficulties can be overcome by  $^{13}\text{C}$ – $^{13}\text{C}$  and for the first time  $^{15}\text{N}$ – $^{13}\text{C}$  correlation experiments, recorded with the help of dynamic nuclear polarization. We present the complete *de novo*  $^{13}\text{C}$  and  $^{15}\text{N}$  resonance assignment at NA of a self-assembled 2'-deoxyguanosine derivative presenting two different molecules in the asymmetric crystallographic unit cell. This *de novo* assignment method is exclusively based on aforementioned correlation spectra and is an important addition to the NMR crystallography approach, rendering firstly  $^1\text{H}$  assignment straightforward, and being secondly a prerequisite for distance measurements with solid-state NMR.

Structure determination of powdered organic solids is of utter importance to understand their properties and function. Their structural investigation poses a particular challenge when single crystal X-ray diffraction (XRD) cannot be applied. The key approach in such cases is so-called NMR crystallography. It combines information from analytical and computational techniques like powder XRD, crystal structure prediction, density functional theory (DFT), and solid-state NMR (ssNMR) to solve or most commonly refine crystal structures of small molecules.<sup>1</sup>

Within this context, most NMR experiments aim at assigning spectral resonances and comparing them to chemical shifts obtained from DFT computations with the gauge invariant projector augmented wave (GIPAW) method.<sup>2</sup> This practice is used to validate a proposed structure or to choose from a set of trial crystal structures the most likely one.<sup>3</sup> In particular,  $^1\text{H}$  chemical shifts have been shown to be very sensitive to crystal packing and thus a good measure for this method.<sup>4,5</sup>

For this reason, but as well because of the much better sensitivity of proton spins compared to  $^{13}\text{C}$  and  $^{15}\text{N}$  (sensitivity

relative to  $^1\text{H}$ :  $1.76 \times 10^{-4}$  and  $3.85 \times 10^{-6}$ , respectively, taking into account their natural isotopic abundance, NA),<sup>6</sup> typical two-dimensional (2D) NMR experiments correlating spins in NMR crystallography display at least one  $^1\text{H}$  spectral dimension.<sup>7</sup>  $^{13}\text{C}$ – $^{13}\text{C}$  or  $^{13}\text{C}$ – $^{15}\text{N}$  correlations are usually out of reach due to the low NA of these spin pairs compared to an isotopically enriched sample ( $\sim 0.01\%$  and  $\sim 0.004\%$ , respectively). Hence, the broad applicability of NMR crystallography is limited by poor proton spectral resolution, even though significant progress has been made on this front over the last few decades.<sup>8,9</sup>

Consequently, a *de novo* resonance assignment is not straightforward especially when spectral ambiguities occur, caused, for example, by peak splitting due to polymorphism or crystallographic asymmetry.<sup>10</sup> In particular, the inability to assign  $^{13}\text{C}$  and  $^{15}\text{N}$  resonances also affects the proton assignment, which is mostly done from H–X correlation spectra. In such instances, tentative assignments, mostly relying on comparisons with DFT results, become necessary. This constitutes a potential source of uncertainties and errors.<sup>10</sup>

In the present work, we show that this limitation can be overcome and report the first complete *de novo*  $^{13}\text{C}$  and  $^{15}\text{N}$  chemical shift assignment of a NA sample with two molecules in the asymmetric crystallographic unit cell. This approach is exclusively based on NMR experimental data, notably involving the first NA  $^{15}\text{N}$ – $^{13}\text{C}$  correlation spectrum. Owing to the high spectral resolution, an unambiguous assignment is straightforward and does not require any previous knowledge of the crystal structure. The incredibly low sensitivity of these experiments is compensated by the use of magic-angle spinning dynamic nuclear polarization (MAS-DNP), which makes them feasible within hours. MAS-DNP relies on the use of *in situ* high-frequency microwave irradiation in order to transfer large intrinsic electron polarization to surrounding nuclei, thereby significantly enhancing their NMR sensitivity.<sup>11,12</sup> It has recently been shown that MAS-DNP can be used to record  $^{13}\text{C}$ – $^{13}\text{C}$  correlation spectra at NA in short experimental times (20 min to a few hours).<sup>13–18</sup>

Received: September 22, 2015

Published: October 20, 2015

This resonance assignment for NMR crystallography using MAS-DNP is demonstrated on 2'-deoxy-3',5'-dipropanoylguanosine ( $dG(C3)_2$ , Figure 1a), a derivative of the DNA base

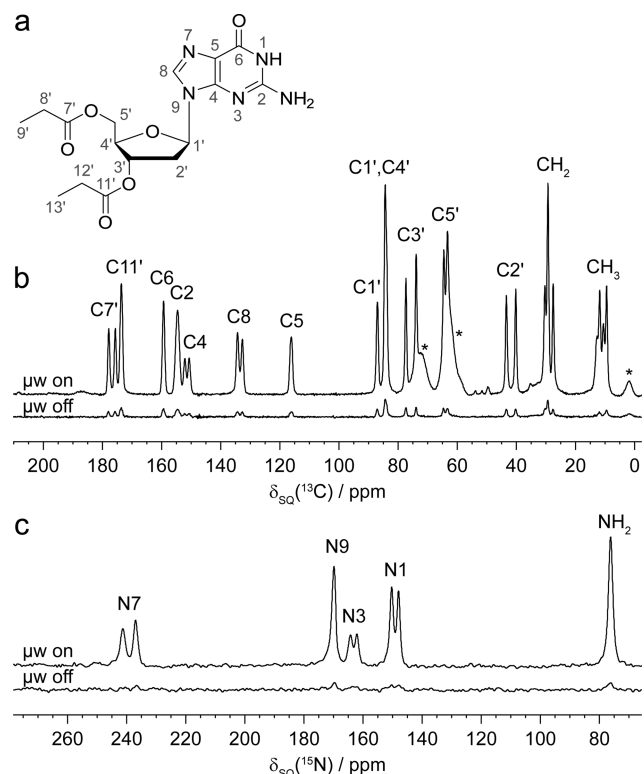


**Figure 1.** Chemical structure of  $dG(C3)_2$  (a) and  $^{13}C$  (b) and  $^{15}N$  (c) CPMAS spectra. Asterisks (\*) indicate glycerol and silicon grease (from sample synthesis and preparation).

deoxyguanosine.<sup>19</sup> Mediated by hydrogen bonding, it self-assembles into a ribbon-like structure in the solid state.<sup>20</sup> It is a representative of the large family of self-assembled guanine-based architectures, with possible applications in fields ranging from medicinal chemistry to nanotechnology.<sup>21–23</sup> Solid guanine-based architectures for instance could be used to fabricate molecular electronic devices like photodetectors and light-harvesting systems.<sup>22–24</sup> Previous ssNMR studies of  $dG(C3)_2$  and related compounds were able to reveal different hydrogen bonding arrangements, which allows to distinguish quartet- and ribbon-like self-assembly.<sup>25,26</sup> However, a full resonance assignment of  $dG(C3)_2$  so far had to rely on GIPAW chemical shift calculations based on the known crystal structure, since separate assignment of the two molecules in the asymmetric unit cell was not possible from NMR alone.<sup>26</sup>

For DNP experiments,  $dG(C3)_2$  (30 mg) was impregnated with a 10 mM solution (30  $\mu$ L) of the biradical AMUPol<sup>27</sup> in  $D_8$ -glycerol/ $D_2O$  (60:40 v/v). The sample had a pasty consistency, did not contain excess liquid, and was fully packed into a 3.2 mm thin-wall zirconia rotor. All DNP experiments were performed on a 9.4 T Bruker AVANCE III wide-bore NMR system equipped with a 263 GHz gyrotron, a transmission line, and a low-temperature ( $\sim$ 100 K) triple-resonance 3.2 mm MAS probe. All spectra were recorded after an initial cross-polarization (CP) step from DNP-enhanced proton spins at an MAS frequency of 12.5 kHz and with a recycle delay of 2.6 s, unless otherwise stated. The sample

temperature was  $\sim$ 105 K. Further experimental details are specified in figure captions and Supporting Information (SI).

DNP-enhanced  $^{13}C$  and  $^{15}N$  CPMAS spectra of  $dG(C3)_2$  are shown in Figure 1b,c. The DNP signal enhancement ( $^{1H}\epsilon_{on/off}$ ) is 11, and an absolute sensitivity ratio (ASR)<sup>13</sup> of  $>10$  was measured, which translates into a time saving factor of at least 100 compared to conventional ssNMR experiments (using a 4 mm rotor at room temperature, RT). The CPMAS spectra at 105 K are consistent with, and of similar resolution, to spectra recorded at RT (see SI), with only minor resonance shifts ( $<2$  ppm) and broader  $CH_3$  contributions occurring. The spectra shown here are very similar to published spectra,<sup>25,26</sup> with our sample presenting the expected ribbon-like structure. Worth noticing are also the remarkably narrow  $^{13}C$  and  $^{15}N$  line widths at 105 K (60–70 Hz for  $^{13}C$  and  $\sim$ 40 Hz for  $^{15}N$  resonances). This is an indicator of a rigid self-assembled structure, but also a result of measuring at NA, where the carbon lines in 1D spectra are not broadened by  $J_{C-C}$  couplings (more than 50 Hz for aromatic carbons).

A striking feature of the CPMAS spectra is the doubling of peaks for the majority of the resonances (differences up to 3.5 ppm for  $C3'$  and 4.4 ppm for  $N7$ ) due to the presence of two distinct molecules (A and B) in the asymmetric unit cell of  $dG(C3)_2$ .<sup>20</sup> This signal splitting makes the acquisition of 2D spectra necessary for complete resonance assignment.

As a first step for  $^{13}C$  resonance assignment, a through-bond  $^{13}C$ – $^{13}C$   $J$ -refocused INADEQUATE<sup>28</sup> spectrum<sup>28</sup> was recorded (Figure 2a). As multiple-bond  $J$ -couplings are very small, the spectrum only shows one-bond contacts, and the unambiguous connection of directly bonded carbon nuclei is possible. This allows the identification of the different  $dG(C3)_2$  subunits for the two conformers, i.e., deoxyribose, the two propanoyl side chains and a part of the guanine base ( $C4$ – $C6$ ). For deoxyribose, signals belonging to molecules A and B can be clearly distinguished (see also Figure S4). However, a connection to other parts of the molecule cannot be made, as the chains of carbon atoms are interrupted by nitrogen or oxygen atoms. Based on this spectrum alone, it is thus not possible to assign the propanoyl and guanine resonances to molecules A and B. In addition, the two propanoyl side chains of one molecule cannot be distinguished.

For this purpose, a through-space  $^{13}C$ – $^{13}C$  correlation spectrum was recorded, employing the dipolar recoupling sequence SR26.<sup>29,30</sup> Importantly, the observation of long distance correlations at appropriate mixing times is facilitated by the lack of dipolar truncation in samples with nuclei at low isotopic abundance.<sup>13,16</sup> Acquired with the DQ-excitation and -reconversion mixing times set each to 2 ms, the spectrum shown in Figure 2b displays both one- and two-bond correlations and allows to complete the  $^{13}C$  assignment. As highlighted in the spectrum, the two propanoyl side chains can be distinguished, and the corresponding resonances assigned through the  $C7'$ – $C5'$  and  $C11'$ – $C3'$  correlations. In addition, the  $C1'$ – $C4$  and  $C1'$ – $C8$  correlations allow for the unambiguous assignment of the split guanine resonances  $C4$  and  $C8$  to molecules A and B. The latter will be confirmed by a  $^{15}N$ – $^{13}C$  double CP-based heteronuclear correlation experiment (DCP-HETCOR) discussed below. The two  $^{13}C$ – $^{13}C$  correlation spectra of Figure 2 thus permit the complete assignment of all  $^{13}C$  resonances of both conformers.

For the assignment of nitrogen resonances, a  $^{15}N$ – $^{13}C$  DCP-HETCOR spectrum of  $dG(C3)_2$  was recorded (Figure 3). To the best of our knowledge, this is the first time such an

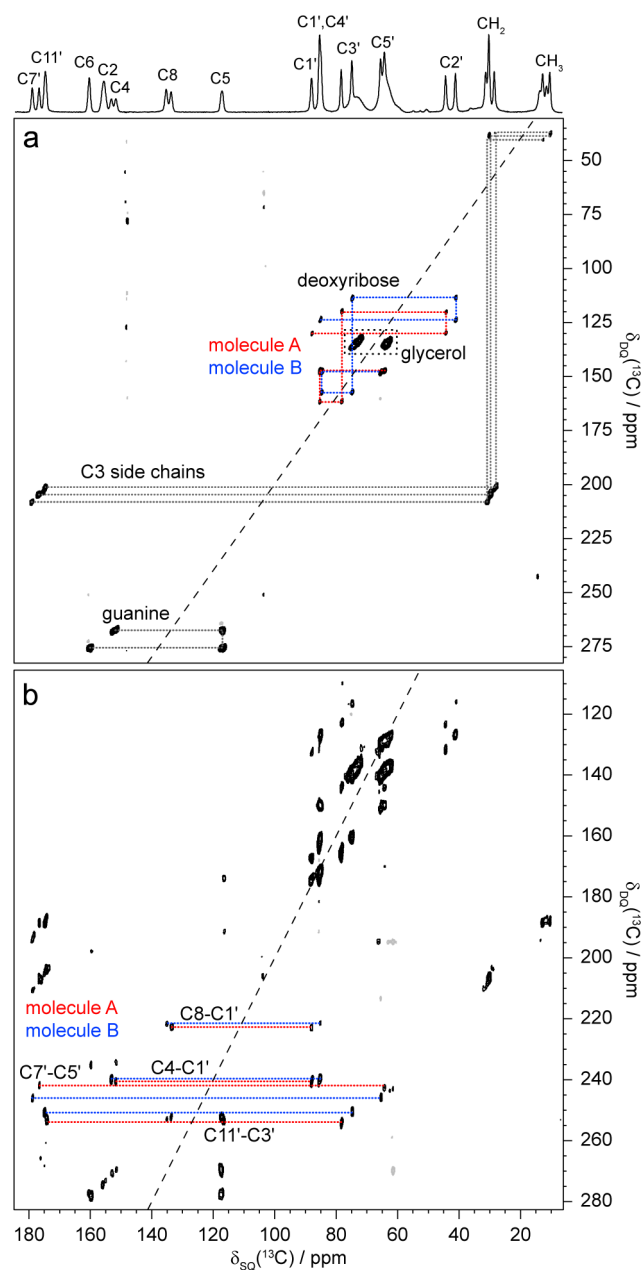


**Figure 2.** (a)  $^{13}\text{C}$ - $^{13}\text{C}$  J-refocused INADEQUATE spectrum<sup>28</sup> of  $\text{dG}(\text{C}3)_2$ . The spectrum was recorded in  $\sim 18$  h. The  $^{13}\text{C}$  CPMAS spectrum is shown above for illustrative purposes. (b)  $^{13}\text{C}$ - $^{13}\text{C}$  DQ-SQ correlation spectrum obtained with the dipolar recoupling sequence SR26<sup>29,30</sup> at 8 kHz MAS frequency. Two spectra were co-added, each taken in  $\sim 7$  h.

experiment has been achieved at NA in ssNMR. The  $^{15}\text{N}$ - $^{13}\text{C}$  CP contact time (7 ms) was chosen such that only one-bond transfers can occur. Despite the very low NA of both nuclei, we demonstrate here the feasibility of a  $^{15}\text{N}$ - $^{13}\text{C}$  correlation spectrum with good signal-to-noise ratio in reasonable experimental time (cf.  $\sim 25$  h instead of  $>100$  days without MAS-DNP). The spectrum clearly shows all expected one-bond correlations. This allows the straightforward assignment of all nitrogen resonances for both conformers, when combined with only the partial  $^{13}\text{C}$  chemical-shift assignment obtained from the J-refocused INADEQUATE spectrum. Indeed, since N9 is linked to C1', which shows a clear splitting for molecules A and B, the assignment of nitrogen resonances for A and B is

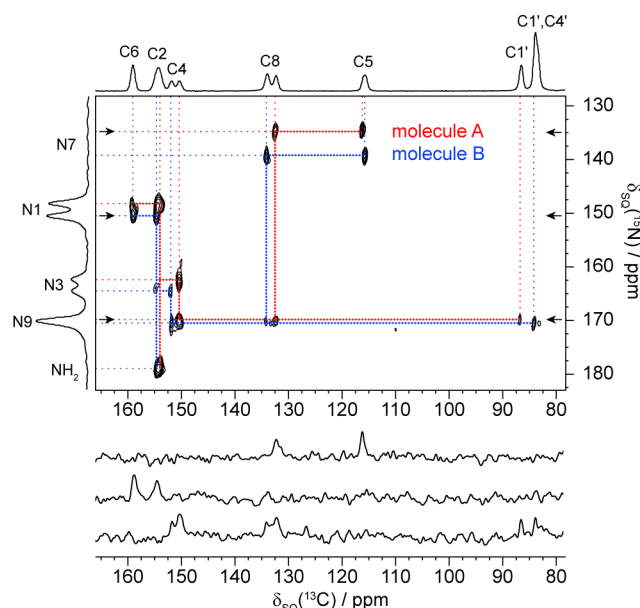


**Figure 3.**  $^{15}\text{N}$ - $^{13}\text{C}$  DCP-HETCOR spectrum of  $\text{dG}(\text{C}3)_2$ .  $^{15}\text{N}$ - $^{13}\text{C}$  polarization transfer was achieved by adiabatic transfer (APHH-CP)<sup>31</sup> with a contact time of 7 ms. The spectrum was recorded in  $\sim 25$  h. The spectral width in the indirect dimension was optimized such that N7 and NH<sub>2</sub> resonances are folded on the respective opposite side of the spectrum.  $^{13}\text{C}$  and  $^{15}\text{N}$  CPMAS spectra are shown above and left for illustrative purposes, respectively. Cross sections are shown below the spectrum, taken at the positions indicated by arrows.

possible. This additionally allows to assign the split C4 and C8 resonances.

Our complete *de novo* assignment of both  $\text{dG}(\text{C}3)_2$  conformers is globally in agreement with previously published GIPAW based results.<sup>26</sup> However, one important discrepancy is found concerning the C7' and C11' resonances of the C3 side chains. Correlation peaks between these carbonyl and the deoxyribose resonances (C7'-C5' and C11'-C3') in the SR26 spectrum clearly show that the carbonyl signals at lower field belong to C7' and those at higher field to C11', which contradicts the computational results used for assignment in ref 26. This carbonyl assignment can also be rationalized on the base of the  $\text{dG}(\text{C}3)_2$  crystal structure: the C7' carbonyl group is involved in a hydrogen bond with the NH<sub>2</sub> group of an adjacent molecule (see Figure S4), which could explain the downfield shift of the C7' resonances with respect to the C11' signal. Moreover, this hydrogen bond seems to present a slightly different length for the two conformations A and B, namely 3.0 and 3.1 Å (O-N distance). This allows the tentative assignment of molecules A and B to the two different conformations in the X-ray structure, with B being the one with the C7' signal at lower field. This again is fully compatible with the GIPAW based assignment (with the aforementioned exception).

To summarize, we have presented the first complete *de novo*  $^{13}\text{C}$  and  $^{15}\text{N}$  resonance assignment of ribbon-like self-assembled  $\text{dG}(\text{C}3)_2$  at NA obtained using DNP-enhanced ssNMR spectroscopy. The assignment was accomplished on the basis of three 2D experiments: a through-bond J-refocused INADEQUATE displaying one-bond  $^{13}\text{C}$ - $^{13}\text{C}$  connections, a through-space homonuclear correlation spectrum based on SR26 dipolar recoupling showing additional longer distance  $^{13}\text{C}$ - $^{13}\text{C}$  correlations, and finally a  $^{15}\text{N}$ - $^{13}\text{C}$  DCP-HETCOR

for assigning the  $^{15}\text{N}$  resonances. Notably, we were able to separately assign the two different molecules in the asymmetric unit cell of  $\text{dG}(\text{C}3)_2$ . This had previously required GIPAW calculations based on the known crystal structure,<sup>26</sup> which however did not yield the fully correct assignment, as shown here. With the assignment of carbon and nitrogen resonances, the assignment of  $^1\text{H}$  chemical shifts using H-X HETCOR experiments becomes straightforward.

The ability to obtain *de novo* (“DFT-free”) NMR assignments at NA is an essential improvement for NMR crystallography, since it does not require prior knowledge of the structure and circumvents potential DFT-based assignment errors. Even more so, the feasibility of performing  $^{13}\text{C}$ – $^{13}\text{C}$  and  $^{15}\text{N}$ – $^{13}\text{C}$  2D correlation experiments at NA is also the crucial first step toward structure determination based on distance measurements, following a similar strategy to the one developed for isotopically enriched biomolecules. In this context, the ability to work at NA also offers a distinctive advantage, since it significantly reduces dipolar truncation effects, paving the way to long distance measurements.<sup>13,16,18</sup> Notably, the inclusion of  $^{15}\text{N}$  will prove particularly useful for investigating structurally essential interactions like hydrogen bonding. With this work, we provide the basis on which these challenging investigations will be conducted.

## ■ ASSOCIATED CONTENT

### 📄 Supporting Information

The Supporting Information is available free of charge on the ACS Publications website at DOI: [10.1021/jacs.5b09964](https://doi.org/10.1021/jacs.5b09964).

Pulse sequences, details of the synthesis and DNP experimental conditions, table of  $^{13}\text{C}$  and  $^{15}\text{N}$  chemical shifts, comparison of 1D spectra at RT and 100 K, full range  $^{13}\text{C}$ – $^{13}\text{C}$  DQ-SQ SR26 spectrum (complement to Figure 2), and illustration of hydrogen bonding in the crystal structure (PDF)

## ■ AUTHOR INFORMATION

### Corresponding Author

\*[gael.depaepe@cea.fr](mailto:gael.depaepe@cea.fr)

### Notes

The authors declare no competing financial interest.

## ■ ACKNOWLEDGMENTS

This work was supported by the French National Research Agency through the “programme blanc” (ANR-12-BS08-0016-01) and the Labex ARCANÉ (ANR-11-LABX-0003-01). Funding from the RTB and the CEA Phare research program (A3DN project) is acknowledged.

## ■ REFERENCES

- (1) *NMR Crystallography*; Harris, R. K., Wasylishen, R. E., Duer, M. J., Eds.; Wiley: Chichester, 2009.
- (2) Pickard, C. J.; Mauri, F. *Phys. Rev. B: Condens. Matter Mater. Phys.* **2001**, *63*, 245101.
- (3) Baías, M.; Dumez, J.-N.; Svensson, P. H.; Schantz, S.; Day, G. M.; Emsley, L. *J. Am. Chem. Soc.* **2013**, *135*, 17501 and references therein.
- (4) Brown, S. P.; Spiess, H. W. *Chem. Rev.* **2001**, *101*, 4125.
- (5) Baías, M.; Widdifield, C. M.; Dumez, J.-N.; Thompson, H. P. G.; Cooper, T. G.; Salager, E.; Bassil, S.; Stein, R. S.; Lesage, A.; Day, G. M.; Emsley, L. *Phys. Chem. Chem. Phys.* **2013**, *15*, 8069.
- (6) Lide, D. R. In *CRC Handbook of Chemistry and Physics*; Haynes, W. M., Ed.; CRC Press: Boca Raton, FL, 2002; chapt. 8, p 49.

- (7) Lesage, A.; Charmont, P.; Steuernagel, S.; Emsley, L. *J. Am. Chem. Soc.* **2000**, *122*, 9739.
- (8) Lesage, A. *Phys. Chem. Chem. Phys.* **2009**, *11*, 6876.
- (9) Madhu, P. K. *Solid State Nucl. Magn. Reson.* **2009**, *35*, 2.
- (10) Harris, R. K.; Hodgkinson, P.; Pickard, C. J.; Yates, J. R.; Zorin, V. *Magn. Reson. Chem.* **2007**, *45*, S174.
- (11) Barnes, A. B.; De Paëpe, G.; Van Der Wel, P. C. A.; Hu, K.-N. N.; Joo, C. G.; Bajaj, V. S.; Mak-Jurkauskas, M. L.; Sirigiri, J. R.; Herzfeld, J.; Temkin, R. J.; Griffin, R. G. *Appl. Magn. Reson.* **2008**, *34*, 237.
- (12) Ni, Q. Z.; Daviso, E.; Can, T. V.; Markhasin, E.; Jawla, S. K.; Swager, T. M.; Temkin, R. J.; Herzfeld, J.; Griffin, R. G. *Acc. Chem. Res.* **2013**, *46*, 1933.
- (13) Takahashi, H.; Lee, D.; Dubois, L.; Bardet, M.; Hediger, S.; De Paëpe, G. *Angew. Chem., Int. Ed.* **2012**, *51*, 11766.
- (14) Rossini, A. J.; Zagdoun, A.; Hegner, F.; Schwarzwälder, M.; Gajan, D.; Copéret, C.; Lesage, A.; Emsley, L. *J. Am. Chem. Soc.* **2012**, *134*, 16899.
- (15) Takahashi, H.; Hediger, S.; De Paëpe, G. *Chem. Commun.* **2013**, 49, 9479.
- (16) Takahashi, H.; Viverge, B.; Lee, D.; Rannou, P.; De Paëpe, G. *Angew. Chem., Int. Ed.* **2013**, *52*, 6979.
- (17) Rossini, A. J.; Widdifield, C. M.; Zagdoun, A.; Lelli, M.; Schwarzwälder, M.; Copéret, C.; Lesage, A.; Emsley, L. *J. Am. Chem. Soc.* **2014**, *136*, 2324.
- (18) Mollica, G.; Dekhil, M.; Ziarelli, F.; Thureau, P.; Viel, S. *Angew. Chem., Int. Ed.* **2015**, *54*, 6028.
- (19) Manet, I.; Francini, L.; Masiero, S.; Pieraccini, S.; Spada, G. P.; Gottarelli, G. *Helv. Chim. Acta* **2001**, *84*, 2096.
- (20) Giorgi, T.; Grepioni, F.; Manet, I.; Mariani, P.; Masiero, S.; Mezzina, E.; Pieraccini, S.; Saturni, L.; Spada, G. P.; Gottarelli, G. *Chem. - Eur. J.* **2002**, *8*, 2143.
- (21) Davis, J. T. *Angew. Chem., Int. Ed.* **2004**, *43*, 668.
- (22) Davis, J. T.; Spada, G. P. *Chem. Soc. Rev.* **2007**, *36*, 296.
- (23) Lena, S.; Masiero, S.; Pieraccini, S.; Spada, G. P. *Chem. - Eur. J.* **2009**, *15*, 7792.
- (24) Pu, F.; Wu, L.; Ran, X.; Ren, J.; Qu, X. *Angew. Chem., Int. Ed.* **2015**, *54*, 892.
- (25) Pham, T. N.; Masiero, S.; Gottarelli, G.; Brown, S. P. *J. Am. Chem. Soc.* **2005**, *127*, 16018.
- (26) Webber, A. L.; Masiero, S.; Pieraccini, S.; Burley, J. C.; Tatton, A. S.; Iuga, D.; Pham, T. N.; Spada, G. P.; Brown, S. P. *J. Am. Chem. Soc.* **2011**, *133*, 19777.
- (27) Sauvée, C.; Rosay, M.; Casano, G.; Aussenac, F.; Weber, R. T.; Ouari, O.; Tordo, P. *Angew. Chem., Int. Ed.* **2013**, *52*, 10858.
- (28) Lesage, A.; Bardet, M.; Emsley, L. *J. Am. Chem. Soc.* **1999**, *121*, 10987.
- (29) Kristiansen, P. E.; Carravetta, M.; Lai, W. C.; Levitt, M. H. *Chem. Phys. Lett.* **2004**, *390*, 1.
- (30) Kristiansen, P. E.; Carravetta, M.; van Beek, J. D.; Lai, W. C.; Levitt, M. H. *J. Chem. Phys.* **2006**, *124*, 234510.
- (31) Baldus, M.; Geurts, D. G.; Hediger, S.; Meier, B. H. *J. Magn. Reson., Ser. A* **1996**, *118*, 140.